 CMC, vol.1, no.2, pp.129-140, 2004

A Meshless Local Petrov-Galerkin (MLPG) Approach for 3-Dimensional Elasto-dynamics

Z. D. Han[1] **and S. N. Atluri**[2]

Abstract: A Meshless Local Petrov-Galerkin (MLPG) method has been developed for solving 3D elasto-dynamic problems. It is derived from the local weak form of the equilibrium equations by using the general MLPG concept. By incorporating the moving least squares (MLS) approximations for trial and test functions, the local weak form is discretized, and is integrated over the local sub-domain for the transient structural analysis. The present numerical technique imposes a correction to the accelerations, to enforce the kinematic boundary conditions in the MLS approximation, while using an explicit time-integration algorithm. Numerical examples for solving the transient response of the elastic structures are included. The results demonstrate the efficiency and accuracy of the present method for solving the elasto-dynamic problems; and its superiority over the Galerkin Finite Element Method.

keyword: Meshless Local Petrov-Galerkin approach (MLPG), Dyanmics, Moving Least Squares (MLS).

1 Introduction

Understanding and controlling structural dynamic response are of great importance, due to their practical applications, especially for impact, contact and penetration problems. Some explicit dynamic FE-codes have been developed as commercial engineering analysis tools, for simulations of such structural- dynamics problems. However, the FEM still has several drawbacks for the simulation, including the quality of the mesh refinement, the element type and order, the hourglass control and so on. Although it has been reported that the simple elements have achieved considerable success for explicit dynamic analysis, the simulation of impact, contact and penetration problems require a much higher accuracy in stresses, which can not be achieved by using the simple elements. Moreover, for higher order elements, the row-sum method of lumping the mass results in zero or negative corner masses.

In contrast, the meshless local Petrov-Galerkin (MLPG) approach has become very attractive, as a promising method for solving 3D problems. The MLPG concept was presented in Atluri and Zhu (1998). The main advantage of this method over the widely used finite element methods is that it does not need any mesh, either for the interpolation of the solution variables or for the integration of the weak forms. It has been developed as a general framework for solving partial differential equations, by Atluri and colleagues [Atluri(2004)]. The MLPG approach has been applied for 2D and 3D domain solutions [Atluri and Zhu (1998), Atluri and Shen (2002a,b), Li, Shen, Han and Atluri (2003), Han and Atluri (2004), Sellountos and Polyzos (2003), Sladek, Sladek and Zhang(2003)], and for boundary integral equations, as the MLPG/BIE method[Atluri, Han and Shen (2003), Han and Atluri (2003a,b)]. After many pioneering research studies were successfully carried out for 2D problems, the MLPG methods are becoming more attractive for solving 3D problems, because of their distinct advantages over the element-based methods. The representative 3D works include the papers of [Li, Shen, Han and Atluri (2003), Han and Atluri (2004)] for 3D elastic problems by using MLPG domain methods, and [Han and Atluri(2003b)] for 3D elastic fracture problem by using MLPG/BIE methods. With a simpler manner for defining the local sub-domains, over the scattered pointed for 3D problems as shown in Han and Atluri(2004), it becomes much easier to handle the local integrals over the intersection of the local sub-domain and the global boundary of the arbitrary 3D solution domain. It makes the MLPG method more practical for solving 3-D problems. In addition, it has been reported that the MLPG methods give better accuracy with

[1] Knowledge Systems Research, LLC
[2] Center for Aerospace Research & Education
University of California, Irvine
5251 California Avenue, Suite 140
Irvine, CA, 92612, USA

lesser CPU time and lesser system resources, than the element-based methods [Atluri and Shen (2002a,b), Han and Atluri (2004)]. It makes the MLPG method to be more efficient, in solving large-scale dynamic problems.

The study in this paper represents a recent effort to develop a 3-D explicit method for solving elasto-dynamic problems by using the MLPG approach. Although some problems can be simplified as the 2-D ones, there are many problems of significance which cannot be described by a two-dimensional geometry, such as the yaw and oblique impacts, contact and penetrations, as well as fragmentation. The present work can easily be enhanced to analyze the large plastic deformations in such nonlinear problems. The present method is based on the local symmetric weak form (LSWF), along with the use of the MLS approximation, in which the shape functions are constructed at the local scattered points with the higher order continuities, which yields more continuous stress fields. One of the major disadvantages of the MLS is that the shape functions do not possess the Kronecker delta property, which makes it difficult to impose the kinematic boundary conditions. However, it becomes easier to handle the kinematic boundary conditions in the dynamic cases, if explicit time-integration schemes are used. A simple procedure for treating the kinematic boundary conditions in transient dynamic problems is presented in the present paper. It renders the present MLPG method to be even more efficient for solving the dynamic problems, than the static ones [as compared to the FEM], because no matrix inversion is required in the explicit scheme. The local sub-domains are constructed at the local scattered points, with the use of the local polyhedrons, as presented in Han and Atluri (2004).

The following discussion begins with the local symmetric weak form of elasto-dynamics, in Section 2. The discretization and the numerical implementation, along with a novel idea for the enforcement of the kinematic boundary conditions are presented in Section 3. Numerical examples for 3D elasto-dynamic problems are given in Section 4. Then paper ends with conclusions and discussions in Section 5.

2 Local symmetric weak-forms (LSWF) of elasto-dynamics

Consider a linear elastic body in a 3D domain Ω, with a boundary $\partial\Omega$. The solid is assumed to undergo infinitesimal deformations. The equations of balance of linear and angular momentum can be written as:

$$\sigma_{ij,j} + f_i - \rho a_i = 0; \quad \sigma_{ij} = \sigma_{ji}; \quad ()_{,i} \equiv \frac{\partial}{\partial \xi_i} \tag{1}$$

where σ_{ij} is the stress tensor, which corresponds to the displacement field u_i, the acceleration field is a_i; and f_i is the body force. The corresponding boundary conditions are given as follows,

$$u_i = \overline{u}_i \ \text{ on } \ \Gamma_u \tag{2a}$$

$$t_i \equiv \sigma_{ij} n_j = \overline{t}_i \ \text{ on } \ \Gamma_t \tag{2b}$$

where $\overline{u}_i$ and $\overline{t}_i$ are the prescribed displacements and tractions, respectively, on the displacement boundary Γ_u and on the traction boundary Γ_t, and n_i is the unit outward normal to the boundary Γ.

The strain-displacement relations are:

$$\varepsilon_{kl} = \frac{1}{2}(u_{k,l} + u_{l,k}) \tag{3}$$

The constitutive relations of an isotropic linear elastic homogeneous solid are:

$$\sigma_{ij} = E_{ijkl}\varepsilon_{kl} = E_{ijkl}u_{k,l} \tag{4}$$

where

$$E_{ijkl} = \lambda\delta_{ij}\delta_{kl} + \mu(\delta_{ik}\delta_{jl} + \delta_{il}\delta_{jk}) \tag{5}$$

with λ and μ being the Lame's constants.

In the local Petrov-Galerkin approaches, one may write a weak form over a local sub-domain Ω_s, which may have a arbitrary shape, and contain the a point $\mathbf{x}$ in question, as shown in Figure 1. A generalized local weak form of the differential equation (1) over a local sub-domain Ω_s, can be written as:

$$\int_{\Omega_s} (\sigma_{ij,j} + f_i - \rho a_i) v_i d\Omega = 0 \tag{6}$$

where u_i and v_i are the trial and test functions, respectively.

By applying the divergence theorem, Eq. (6) may be rewritten in a symmetric weak form as:

$$\int_{\partial\Omega_s} \sigma_{ij} n_j v_i d\Gamma - \int_{\Omega_s} (\sigma_{ij} v_{i,j} - f_i v_i + \rho a_i) d\Omega = 0 \tag{7}$$

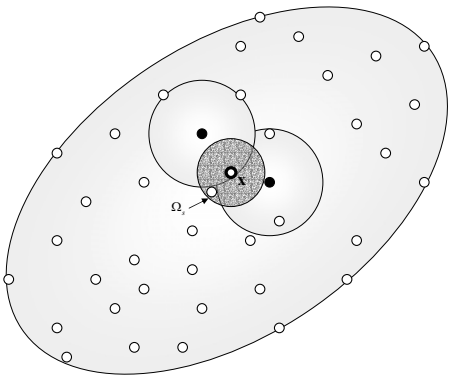

Figure 1 : a local sub-domain around point **x**

Imposing the boundary conditions in (2), one obtains

$$\int_{L_s} t_i v_i d\Gamma + \int_{\Gamma_{su}} t_i v_i d\Gamma + \int_{\Gamma_{st}} \bar{t}_i v_i d\Gamma - \int_{\Omega_s} (\sigma_{ij} v_{i,j} - f_i v_i - \rho a_i) d\Omega = 0 \quad (8)$$

where Γ_{su} is a part of the boundary $\partial\Omega_s$ of Ω_s, over which the essential boundary conditions are specified. In general, $\partial\Omega_s = \Gamma_s \cup L_s$, with Γ_s being a part of the local boundary located on the global boundary and L_s being the other part of the local boundary which is inside the solution domain. $\Gamma_{su} = \Gamma_s \cap \Gamma_u$ is the intersection between the local boundary $\partial\Omega_s$ and the global displacement boundary Γ_u; $\Gamma_{st} = \Gamma_s \cap \Gamma_t$ is a part of the boundary over which the natural boundary conditions are specified.

Therefore, a local symmetric weak form (LSWF) in linear elastodynamics can be written as:

$$\int_{\Omega_s} \sigma_{ij} v_{i,j} d\Omega - \int_{L_s} t_i v_i d\Gamma - \int_{\Gamma_{su}} t_i v_i d\Gamma + \int_{\Omega_s} \rho a_i v_i d\Omega = \int_{\Gamma_{st}} \bar{t}_i v_i d\Gamma + \int_{\Omega_s} f_i v_i d\Omega \quad (9)$$

It requires the special treatment for the essential (kinematic) boundary conditions in the MLPG method for the static problems, because the displacement field along the boundary is not only dependent on the boundary nodes also those inside the solution domain. This topic has been well studied for static problems, by using both the modified collocation method and the penalty method [Zhu and Atluri (1998)]. However, the kinematic b.c can be simply treated by reconditioning the accelerations, if explicit algorithms for the time integration are used. This method is detailed in the next section.

3 Dynamic analysis

3.1 Numerical discretization of the LSWF

To solve the local symmetric weak form in Eq. (9), a local approximation is required and the moving lease squares approach is used in the present study [Atluri and Zhu (1998)]. With the MLS, the distribution of function u in Ω_s can be approximated as,

$$u(\mathbf{x}) = \mathbf{p}^T(\mathbf{x})\mathbf{a}(\mathbf{x}) \quad \forall \mathbf{x} \in \Omega_s \quad (10)$$

where $\mathbf{p}^T(\mathbf{x}) = [p_1(\mathbf{x}), p_2(\mathbf{x}), \ldots, p_m(\mathbf{x})]$ is a monomial basis of order m; and $\mathbf{a}(\mathbf{x})$ is a vector containing coefficients, which are functions of the global Cartesian coordinates $[x_1, x_2, x_3]$, depending on the monomial basis. After minimizing a weighted discrete L_2 norm, one may obtain the approximation from the nodal values at the local scattered points, as [Atluri and Zhu (1998)]

$$u(\mathbf{x}) = \mathbf{\Phi}^T(\mathbf{x})\hat{\mathbf{u}} \quad \forall \mathbf{x} \in \partial\Omega_x \quad (11)$$

where $\mathbf{\Phi}(\mathbf{x})$ is the so-called shape function of the MLS approximation. In the present study, these shape functions are applied to approximate both the displacement and acceleration fields.

We apply the local symmetric weak form in Eq. (9) on the local 3D sub-domain Ω_s, centered on each nodal point $\mathbf{x}^{(I)}$. By taking the shape function of node I in Eq. (11), $\Phi^{(I)}(\mathbf{x})$, as the test function, and choosing the local-domain to be the same as the support domain of the node, Eq. (9) can be simplified for $u_i^{(I)}$ as:

$$\int_{\Omega_s} \sigma_{ij} \Phi^{(I)}_{,j} d\Omega - \int_{\Gamma_{su}} t_i \Phi^{(I)} d\Gamma + \int_{\Omega_s} \rho a_i \Phi^{(I)} d\Omega = \int_{\Gamma_{st}} \bar{t}_i \Phi^{(I)} d\Gamma + \int_{\Omega_s} f_i \Phi^{(I)} d\Omega \quad (12)$$

in which the following condition has been used:

$$\Phi^{(I)}(\mathbf{x}) = 0 \qquad for \quad \forall \mathbf{x} \in L_s \quad (13)$$

3.2 Enforcement of essential (kinematic) boundary conditions

It is well known that the MLS approximation gives the shape functions based on the virtual nodal values,

which do not possess the Kronecker delta property. The compactly-supported radius basis functions (CRBF) may construct the shape functions with such a property. However, it has been reported [Han and Atluri(2004)], that the shape functions from the CRBF are non-continuous when the CRBF is used locally. In addition, the fields on the boundary, where kinematic b.c are prescribed, are not only dependent on the nodal values located on the boundary but also on those inside the solution domain. They are also not linear between the boundary nodes. From the numerical point of view, if the kinematic boundary conditions are enforced strictly along the entire essential boundary, it will introduce too many constraints to the internal nodes. It makes the structure much stiffer. In the present study, the standard collocation method is enhanced for the explicit dynamic analysis.

For the nodes which belong to the essential boundary, i.e., $u_i^{(I)} \in \Gamma_{su}$, one may take the Derac's delta function as the test function and obtain the corresponding local weak form from Eq. (9), as the standard collocation method, as

$$u_i(\mathbf{x}^{(I)}) = \overline{u}_i(\mathbf{x}^{(I)}) \tag{14}$$

which can be used to enforce the initial essential boundary conditions. Therefore, one may set the corresponding accelerations $\hat{\mathbf{a}}$ to be zero for the nodes belong to the essential boundary. Similar equations can be written for the accelerations as,

$$a_i(\mathbf{x}^{(I)}) = 0 \tag{15}$$

or in the matrix form

$$\mathbf{H}^T \cdot \hat{\mathbf{a}} = 0 \tag{16}$$

After orthogonalizing the matrix $\mathbf{H}$, Eq. (16) can be written in an equivalent form as

$$\mathbf{G}^T \cdot \hat{\mathbf{a}} = 0 \tag{17}$$

and the matrix $\mathbf{G}$ satisfies

$$\mathbf{G}^T \cdot \mathbf{G} = \mathbf{I} \tag{18}$$

where $\mathbf{I}$ is the identity matrix.

One may re-write the system equations in the matrix form after the local weak form in Eq. 3.2 is numerically integrated over each local sub-domain [Han and Atluri (2004)], as

$$\mathbf{M} \cdot \hat{\mathbf{a}} + \mathbf{K} \cdot \hat{\mathbf{u}} = \hat{\mathbf{f}} \tag{19}$$

where the mass matrix, $\mathbf{M}$, is diagonal when the node mass is lumped. With a general explicit time-integration, the accelerations are obtained from Eq. 3.3 as,

$$\hat{\mathbf{a}}' = \mathbf{M}^{-1} \cdot (\hat{\mathbf{f}} - \mathbf{K} \cdot \hat{\mathbf{u}}) \tag{20}$$

With the consideration of the essential boundary conditions in Eq. (17), the accelerations can be corrected to enforce the essential boundary conditions, as

$$\hat{\mathbf{a}} = \hat{\mathbf{a}}' - \mathbf{G} \cdot \mathbf{G}^T \cdot \hat{\mathbf{a}}' \tag{21}$$

3.3 Time integration

The Newmark β method [Newmark (1959)], well known and commonly applied in computations, is used in the present study to integrate the governing equations in time. With the use of Eq. (21) to determine the accelerations, the displacements and velocities are calculated from the standard Newmark β method, as

$$\begin{aligned} \mathbf{u}^{t+\Delta t} &= \mathbf{u}^t + \Delta t\, \mathbf{v}^t + \frac{\Delta t^2}{2}\left[(1-2\beta)\mathbf{a}^t + 2\beta \mathbf{a}^{t+\Delta t}\right] \\ \mathbf{v}_c^{t+\Delta t} &= \mathbf{v}^t + \Delta t\left[(1-\gamma)\mathbf{a}^t + \gamma \mathbf{a}^{t+\Delta t}\right] \end{aligned} \tag{22}$$

For zero damping system, this method is unconditionally stable if

$$2\beta \geq \gamma \geq \frac{1}{2} \tag{23}$$

and conditionally stable if

$$\gamma \geq \frac{1}{2}, \quad \beta \leq \frac{1}{2} \quad \text{and} \quad \Delta t \leq \frac{1}{\omega_{\max}\sqrt{\gamma/2-\beta}} \tag{24}$$

where $\omega_{\max}$ is the the maximum frequency in the structural system.

This method can be used in the predictor-corrector way. After specifying the initial conditions, the time integrations for each time increment can be done in the following steps.

Step 1: predict the displacements and velocities

$$\begin{aligned} \hat{\mathbf{u}}_c^{t+\Delta t} &= \hat{\mathbf{u}}^t + \Delta t\, \hat{\mathbf{v}}^t + \frac{\Delta t^2}{2}(1-2\beta)\hat{\mathbf{a}}^t \\ \hat{\mathbf{v}}_c^{t+\Delta t} &= \hat{\mathbf{v}}^t + \Delta t\,(1-\gamma)\hat{\mathbf{a}}^t \end{aligned} \tag{25}$$

Step 2: predict the acceleration

$$\begin{aligned} \hat{\mathbf{a}}_{c1}^{t+\Delta t} &= \mathbf{M}^{-1} \cdot (\hat{\mathbf{f}}^{t+\Delta t} - \mathbf{K} \cdot \hat{\mathbf{u}}_c^{t+\Delta t}) \\ \hat{\mathbf{a}}_{c2}^{t+\Delta t} &= \hat{\mathbf{a}}_{c1}^{t+\Delta t} - \mathbf{G} \cdot \mathbf{G}^T \cdot \hat{\mathbf{a}}_{c1}^{t+\Delta t} \end{aligned} \tag{26}$$

Step 3: correct the displacements and velocities

$$\hat{\mathbf{u}}^{t+\Delta t} = \hat{\mathbf{u}}_c^{t+\Delta t} + \Delta t^2 \beta \hat{\mathbf{a}}_{c2}^{t+\Delta t}$$
$$\hat{\mathbf{v}}^{t+\Delta t} = \hat{\mathbf{v}}_c^{t+\Delta t} + \Delta t \gamma \hat{\mathbf{a}}_{c2}^{t+\Delta t}] \tag{27}$$

Step 4: correct the acceleration

$$\hat{\mathbf{a}}_{c3}^{t+\Delta t} = \mathbf{M}^{-1} \cdot (\hat{\mathbf{f}}^{t+\Delta t} - \mathbf{K} \cdot \hat{\mathbf{u}}^{t+\Delta t})$$
$$\hat{\mathbf{a}}^{t+\Delta t} = \hat{\mathbf{a}}_{c3}^{t+\Delta t} - \mathbf{G} \cdot \mathbf{G}^T \cdot \hat{\mathbf{a}}_{c3}^{t+\Delta t} \tag{28}$$

The central difference scheme is used in the present study by setting $\beta = 0, \quad \gamma = \frac{1}{2}$. The corresponding time integration is be simplified into the fewer steps as,

$$\hat{\mathbf{u}}^{t+\Delta t} = \hat{\mathbf{u}}^t + \Delta t \hat{\mathbf{v}}^t + \frac{\Delta t^2}{2} \hat{\mathbf{a}}^t$$
$$\hat{\mathbf{a}}_{c1}^{t+\Delta t} = \mathbf{M}^{-1} \cdot (\hat{\mathbf{f}}^{t+\Delta t} - \mathbf{K} \cdot \hat{\mathbf{u}}^{t+\Delta t})$$
$$\hat{\mathbf{a}}^{t+\Delta t} = \hat{\mathbf{a}}_{c1}^{t+\Delta t} - \mathbf{G} \cdot \mathbf{G}^T \cdot \hat{\mathbf{a}}_{c1}^{t+\Delta t}$$
$$\hat{\mathbf{v}}^{t+\Delta t} = \hat{\mathbf{v}}^t + \frac{\Delta t}{2} [\hat{\mathbf{a}}^t + \hat{\mathbf{a}}^{t+\Delta t}] \tag{29}$$

The scheme is conditionally stable, from Eq. 4, if

$$\Delta t \leq \frac{T_{\min}}{\pi} \tag{30}$$

where $T_{\min}$ is the minimum system period.

In the present study, the impact load is simulated to demonstrate the present MLPG method. A smaller time step is required to track the transient response of solid structures. Longitudinal wave speed is used to determine the time step based on the minimum nodal distance.

4 Numerical Examples

Several problems in three-dimensional linear elasto-dynamics are solved to illustrate the effectiveness of the present method. The numerical results of the present methods, as applied to problems in *3D elasto-dynamics*, specifically (i) a cantilever beam, (ii) a concentrated point load on a semi-infinite space (Boussinesq Problem), are discussed.

4.1 Cantilever beam

The performances of the present MLPG formulations are also evaluated, using a three dimensional cantilever beam under uniform tension and transverse loading, as shown in Figure 2. The beam is modeled as the plane stress case with $E = 1 \times 10^6$, $\upsilon = 0.25$, $b = h = 2$, and $L = 24$.

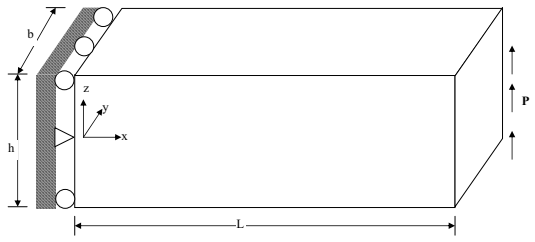

Figure 2 : A cantilever beam with an end load

This problem has been solved by Han and Atluri (2004) in the static case. The results showed that the MLPG methods gave accurate results even with a coarse nodal configuration. As an extension of the static analysis, the beam is modeled with a uniform nodal configuration with a nodal distance, d, of 1.0, as shown in Figure 3. The number of nodes is 225. For comparison purposes, FE meshes are also constructed from the same nodal configuration by using the Hex 8 element for the commercial FE code, NASTRAN.

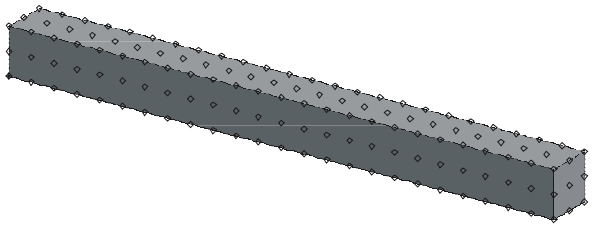

Figure 3 : nodal configuration for a cantilever beam with 225 nodes (nodal distance d=1.0)

The first load is a uniform constant tension applied to the free end of the beam. The problem is solved by using the present MLPG method for the first 0.5 seconds, with 1000 time steps. The dynamic response is obtained and shown in Figure 4, as a typical stationary structural vibration. The same problem is also solved by using NASTRAN. A good agreement is obtained while both results are compared in Figure 4.

The MLPG is used to solve the problem of a beam under the uniform constant transverse load. The dynamic response during the first 5 seconds is simulated, using 5000 time steps. The results of the present MLPG method are shown in Figure 5 with a gray stream line. It can be seen

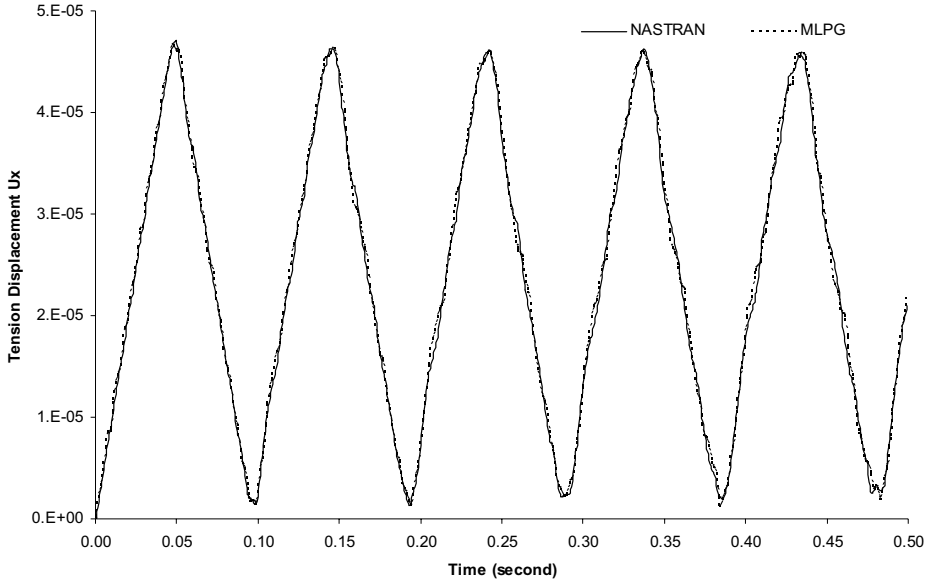

Figure 4 : Structural Response of a cantilever beam under a sudden uniform tension: nodal distance d=1.0, support size R = 2.6

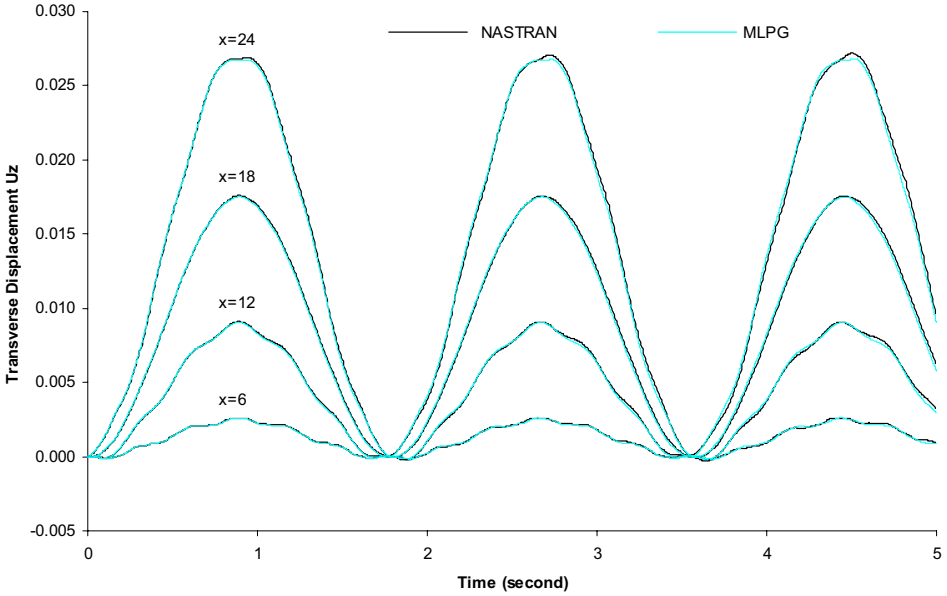

Figure 5 : Structural Response of a cantilever beam under a sudden transverse load: nodal distance d=1.0, support size R = 2.6

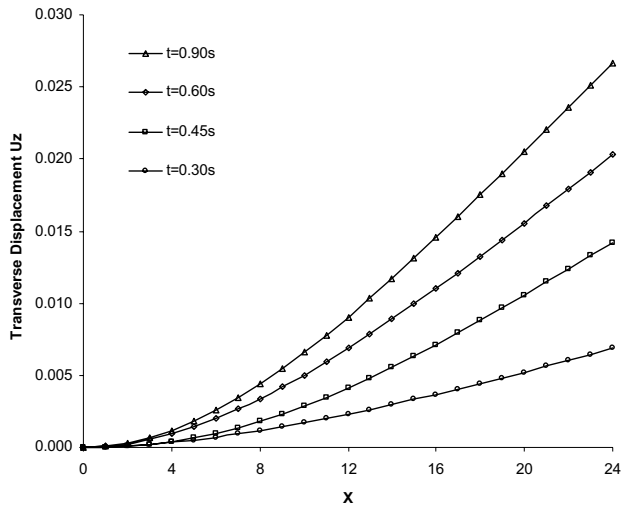

Figure 6 : Structural deformation of a cantilever beam under a sudden transverse load by using the present MLPG method: nodal distance d=1.0, support size R = 2.6

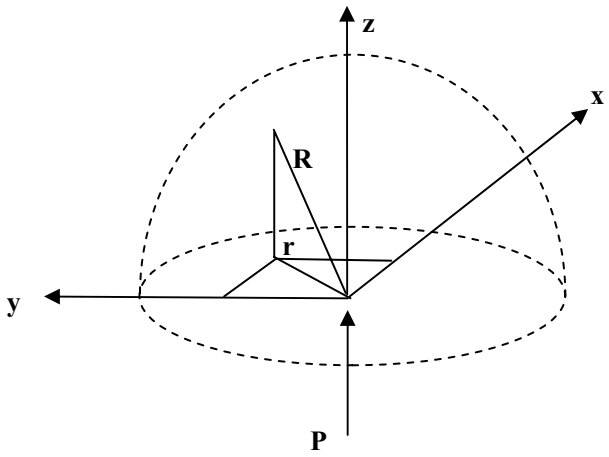

Figure 7 : A concentrated load on a semi-infinite space (Boussinesq Problem)

that results agree well with those obtained by using NASTRAN. Again, it shows a stationary structural vibration in the transverse mode, with lower natural frequencies. The transverse deformations at different times are shown in Figure 6.

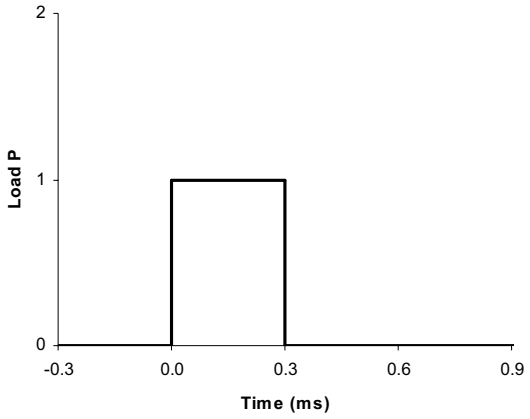

Figure 8 : a pulse load

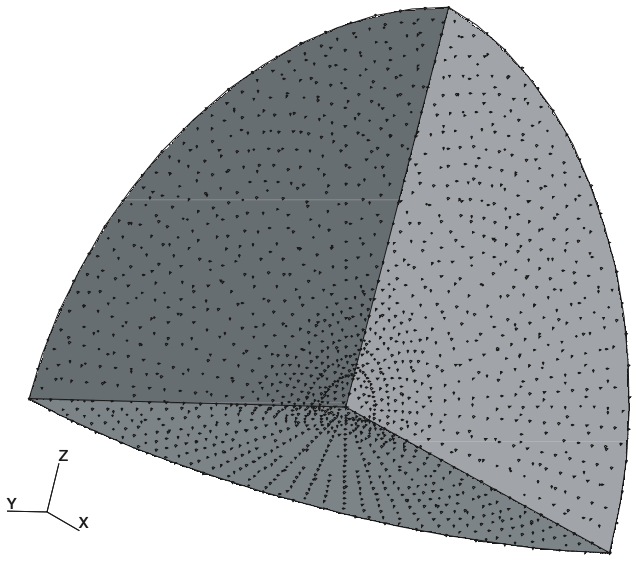

Figure 9 : a non-uniform nodal configuration for the Boussinesq Problem (6862 nodes)

4.2 A concentrated load on a semi-infinite space (Boussinesq problem)

The Boussinesq problem can simply be described as a concentrated load acting on a semi-infinite elastic medium with no body force, as shown in Figure 7. This problem was solved by using MLPG/Heaviside [Li, Shen, Han and Atluri (2003), Han and Atluri (2004)] and MLPG/BIE [Han and Atluri (2003)b] with a static point load. We solve this problem here with a short pulse load (Figure 8), which lasts only for 0.3 milliseconds. This example has been chosen , to demonstrate the capabil-

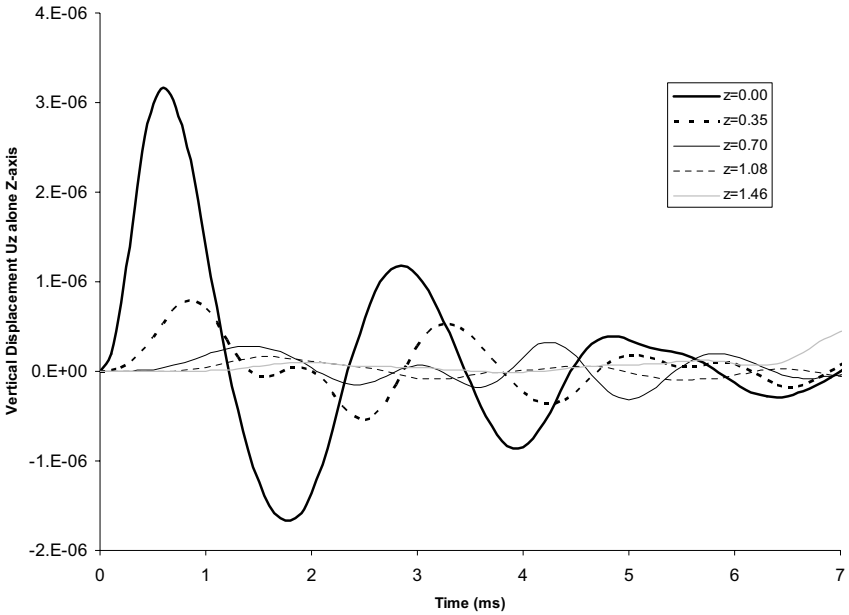

Figure 10 : Transient vertical displacement along z-axis for the Boussinesq problem under a pulse load

ity of the present MLPG method to track the shock wave propagation, when strong singularities are also present. A quarter of a half sphere with a radius of 10 is used to simulate the semi-infinite space, with the consideration of the symmetrical boundary conditions. Young's modulus and Poisson's ratio are chosen to be 1×10^6 and 0.25, respectively. It is modeled with a nodal configuration, as shown in Figure 9, containing 6862 nodes. It should be pointed out that a finer nodal configuration is required in the whole model, to track the shock wave, unlike the coarser nodal configuration which can be used in the area far away from the loading point, as in the static analysis.

The present MLPG method is used to simulate the transient response during the first 7 milliseconds with a time increment of 0.01 millisecond. The transient responses of the nodes along the Z-axis under the shock force are shown in Figure 10, and those along the X-axis and Y-axis in Figure 11 and Figure 12, respectively. It shows clearly that how the energy is transmitted from the loading point to the semi-half space. It can be seen that the transient response of the nodes on the Z-axis occurs at earlier times, than that of the nodes on the X and Y axes. The shock wave propagations along the Z and X axes are shown in Figure 13 and Figure 14 every 0.5 millisecond. From Figure 13, the shock wave along the Z-axis reaches the node at Z=6.78 at a time of 6 milliseconds. From Figure 14, the shock wave along the X-axis reaches the node at X=4.10 at time 6 milliseconds, which is slower than it along the Z-axis. The speeds of the shear and longitudinal waves of the medium used in the present study are 632 m/s and 1092 m/s, respectively. For 6 milliseconds, they propagate 3.79 and 6.55 meters, respectively. From the results, a longitudinal wave is propagating along the Z-axis and a shear wave along the X-axis, while the numerical results show that these responses occur a little bit ahead in time, because of the nodal support size for the MLS.

From these results, it is seen that the present MLPG method gives a good approximation to the transient response, under the pulse loading, even when strong singularities are present. Such pulse loads may occur during impact, contact and penetration events. In the present study, no mesh is required, which avoids the difficulties associated with mesh distortion for the element-based methods, such as the conventional FEM. The present MLPG method simulates the shock-wave problem straightforwardly, without any special numerical techniques, such as reduced integration schemes for avoiding shear-locking, stablizing viscosity (or so-called hour glass control), and so on. In addition, the smoother stress and strain fields can be calculated from the displacements, which give better prediction for the possible

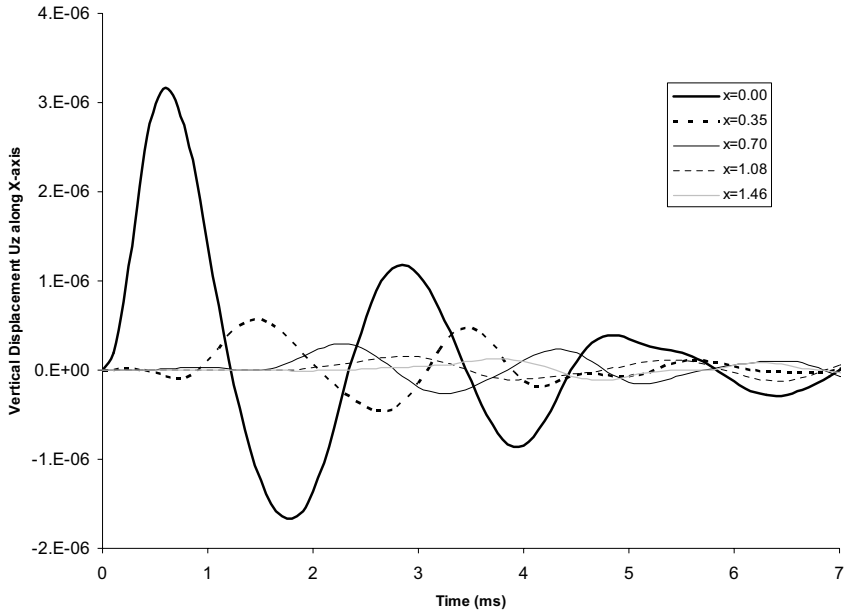

Figure 11 : Transient vertical displacement along x-axis for the Boussinesq problem under a pulse load

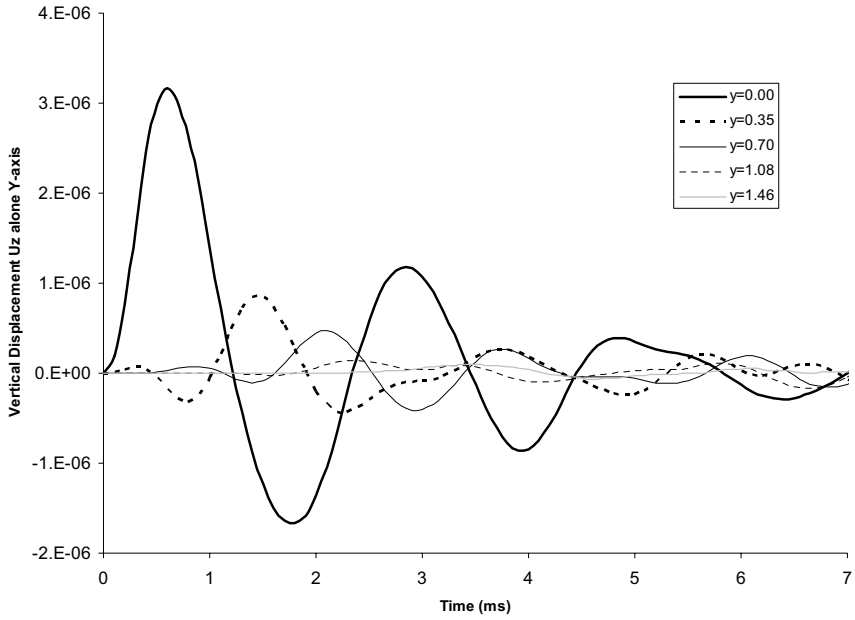

Figure 12 : Transient vertical displacement along y-axis for the Boussinesq problem under a pulse load

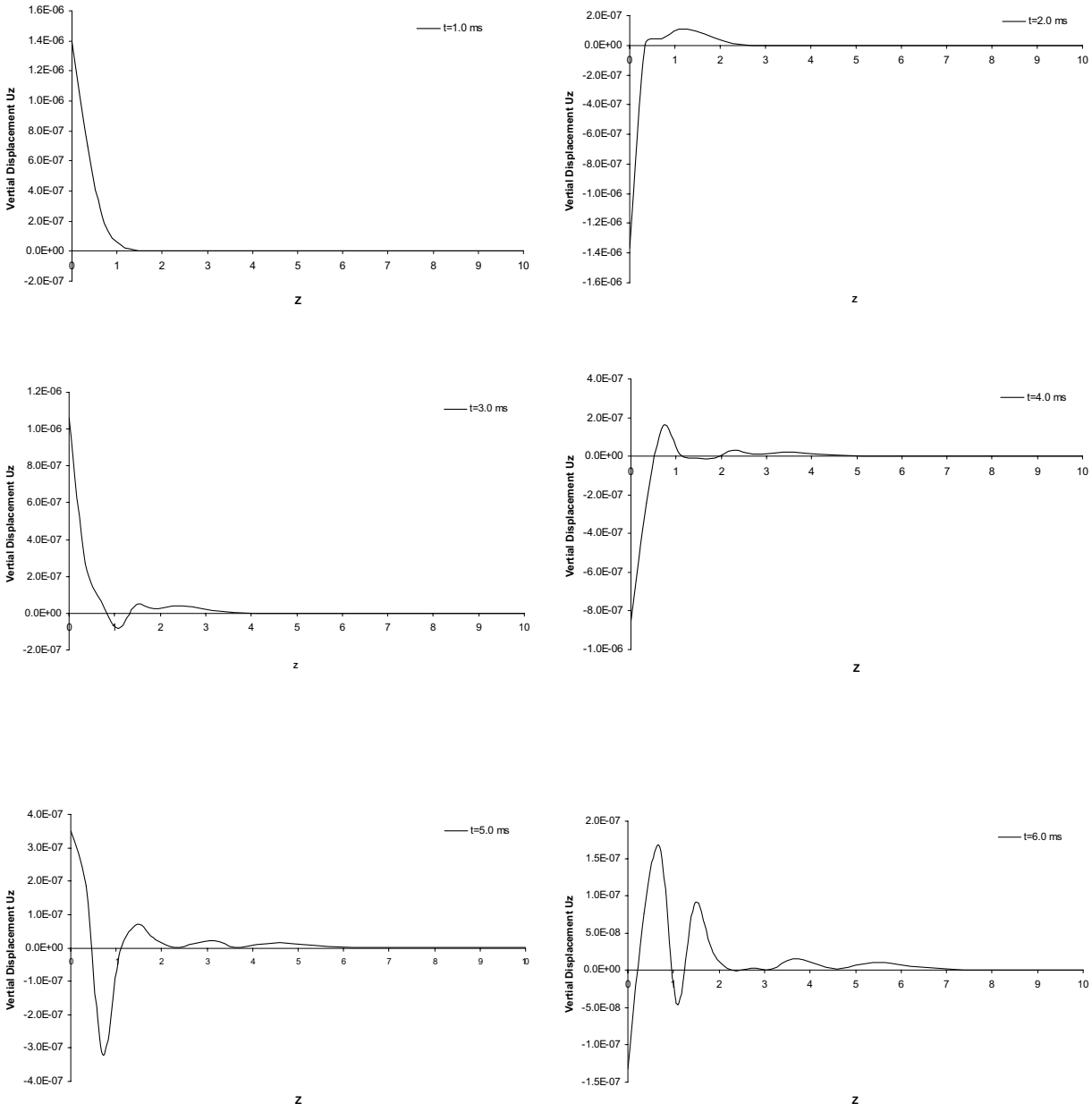

Figure 13 : Transient vertical displacement along z-axis for the Boussinesq problem under a pulse load

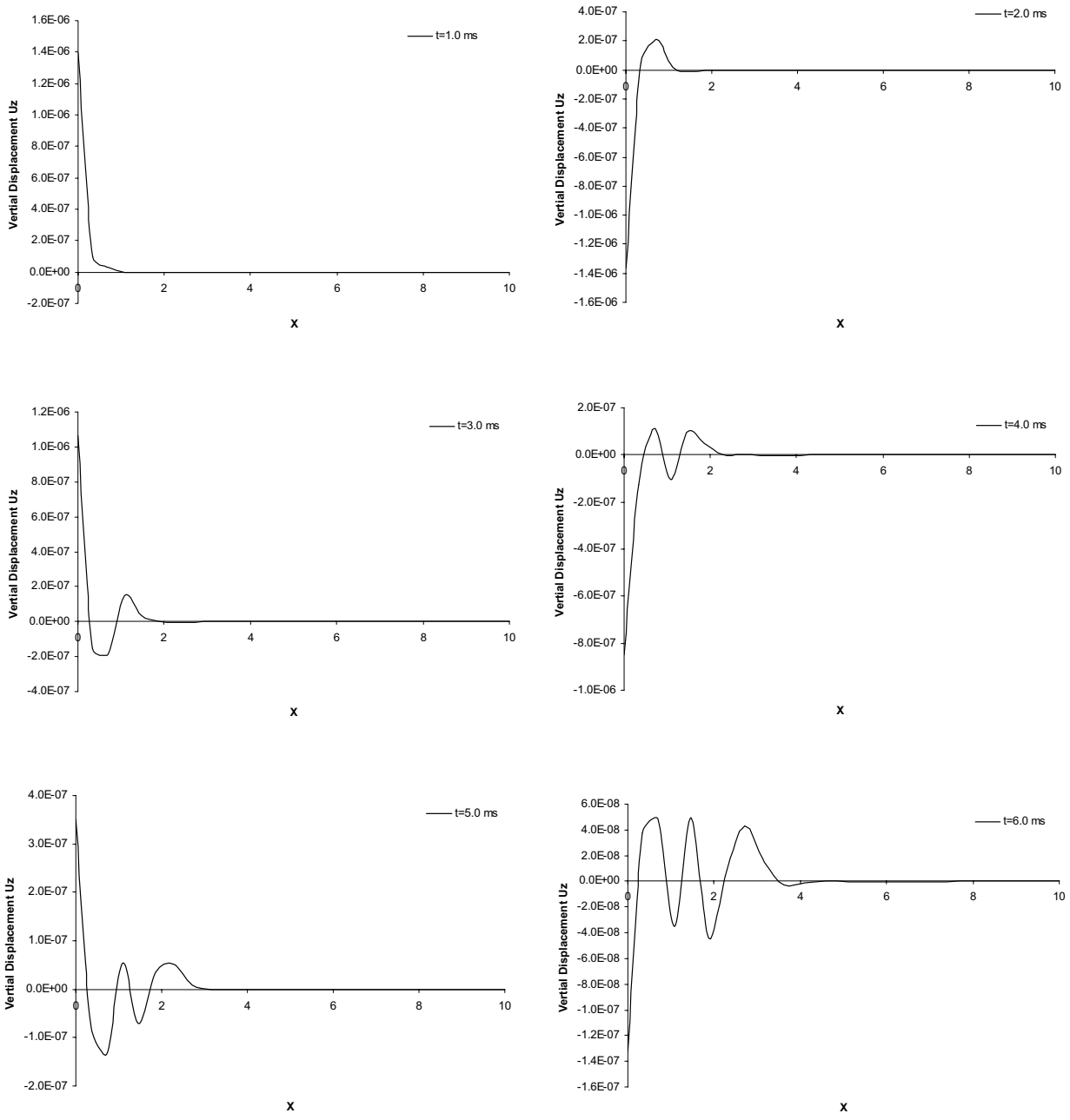

Figure 14 : Transient vertical displacement along x-axis for the Boussinesq problem under a pulse load

crack initialization. With the use of the simpler node adaptation procedures in the meshless methods, crack propagations can be simulated, and fragmentation events can be treated more easily.

5 Closure

A Meshless Local Petrov Galerkin (MLPG) method is developed for 3D dynamic problems, based on the local symmetric weak form (LSWF). The MLS is used for constructing the shape functions at the scattered points. Incorporating with the central difference scheme for time integration, a numerical treatment is developed for the enforcement of the kinematic boundary conditions, which is very effective, computationally. The numerical examples show the capability of the present MLPG method for simulating both the low frequency structural responses, as well as the high-speed shock wave propagations. It can be concluded that the present MLPG method has many distinct advantages, over the element-based methods for the dynamic problems, especially for those with the strong singularities, including contact, penetration, crack initiation and propagation.

Acknowledgement: The results presented in this paper were obtained during the course of investigations supported by the United States Army, under the SBIR Contract, Number: W911NF-04-C-0022. ZH and SNA gratefully acknowledge the fruitful discussions with, and the encouragement received from, Dr. Ellen Segan of the US Army Research Office, during the performance of this research.

References

Atluri, S. N. (2004): *The Meshless Local Petrov-Galerkin (MLPG) Method for Domain & Boundary Discretizations,* Tech Science Press, 665 pages

Atluri, S. N.; Han, Z. D.; Shen, S. (2003): Meshless Local Patrov-Galerkin (MLPG) approaches for weakly-singular traction & displacement boundary integral equations, *CMES: Computer Modeling in Engineering & Sciences*, vol. 4, no. 5, pp. 507-517.

Atluri, S. N.; Shen, S. (2002a): The meshless local Petrov-Galerkin (MLPG) method. Tech. Science Press, 440 pages.

Atluri, S. N.; Shen, S. (2002b): The meshless local Petrov-Galerkin (MLPG) method: A simple & less-costly alternative to the finite element and boundary element methods. *CMES: Computer Modeling in Engineering & Sciences*, vol. 3, no. 1, pp. 11-52

Atluri, S. N.; Zhu, T. (1998): A new meshless local Petrov-Galerkin (MLPG) approach in computational mechanics. *Computational Mechanics.*, Vol. 22, pp. 117-127.

Han. Z. D.; Atluri, S. N. (2003a): On Simple Formulations of Weakly-Singular Traction & Displacement BIE, and Their Solutions through Petrov-Galerkin Approaches, *CMES: Computer Modeling in Engineering & Sciences*, vol. 4 no. 1, pp. 5-20.

Han. Z. D.; Atluri, S. N. (2003b): Truly Meshless Local Petrov-Galerkin (MLPG) Solutions of Traction & Displacement BIEs, *CMES: Computer Modeling in Engineering & Sciences*, vol. 4 no. 6, pp. 665-678.

Han, Z. D.; Atluri, S. N. (2004): Meshless Local Petrov-Galerkin (MLPG) approaches for solving 3D Problems in elasto-statics, *CMES: Computer Modeling in Engineering & Sciences*, (submitted).

Li, Q.; Shen, S.; Han, Z. D.; Atluri, S. N. (2003): Application of Meshless Local Petrov-Galerkin (MLPG) to Problems with Singularities, and Material Discontinuities, in 3-D Elasticity, *CMES: Computer Modeling in Engineering & Sciences*, vol. 4 no. 5, pp. 567-581.

Newmark, N. M. (1959): A method of computation for structural dynamics, *Journal of the Engineering Mechanics Division, ASCE*, vol. 85, pp. 67-94.

Sellountos, E. J.; Polyzos, D. (2003): A MLPG (LBIE) method for solving frequency domain elastic problems, *CMES: Computer Modeling in Engineering & Sciences*, vol. 4, no. 6, pp. 619-636

Sladek, J.; Sladek, V.; Zhang, C. (2003): Application of Meshless Local Petrov-Galerkin (MLPG) Method to Elastodynamic Problems in Continuously Nonhomogeneous Solids, *CMES: Computer Modeling in Engineering & Sciences*, vol. 4, no. 6, pp. 637-648.